Chemical Engineering Science 60 (2005) 589–598

Chemical Engineering Science

www.elsevier.com/locate/ces

Optical technique DPIV in measurements of granular material flows, Part 1 of 3—plane hoppers

I. Sielamowicz[a,*], S. Blonski[b], T.A. Kowalewski[b]

[a] *Technical University, 15-351 Bialystok, Wiejska 45E, Poland*
[b] *Institute of Fund. Technological Research, Polish Academy of Sciences, 00-049 Warsaw, Swietokrzyska 21, Poland*

Received 25 May 2004; received in revised form 22 July 2004; accepted 28 July 2004

Abstract

The aim of this paper is to present the evolution of plug flow developing in three densely packed granular materials in the model of a hopper made of Plexiglas. For this purpose, the digital particle image velocimetry (DPIV) technique is applied to analyse the flow field of the granular material. When discharge starts, a plug flow zone in the flowing material expands upward. This zone changes its width reaching the upper surface of the material. The plug flow evolution as a function of time is described using DPIV. This technique yields the velocity profiles of flowing granular materials, velocity magnitude contours, vector fields, velocity distributions on certain levels in the model and traces of the selected particles. The results obtained for the evolution of the vertical velocity, height and width of the plug flow zone as a function of time, measured at the symmetry axis of the model for the amarantus seed are compared to the results obtained by Waters and Drescher. Measurements of the stagnant boundary as a function of time are compared to the results available in the literature.

Keywords: Optical technique; Experiments; Granular; Materials; Flow; Particle; Plug flow

1. Introduction

Jenike in his reports, published in 1961 and 1964, presented two types of flow during the discharge of granular material from hoppers: mass flow and funnel flow. Watson and Rotter (1996) classified funnel flow into semi-mass flow and internal or pipe flow. The flow channel boundary is also defined as the interface between flowing and stationary solid. The methods based on the concepts of plasticity can predict the existence of stagnant zones but there are no reliable methods for predicting the shape of the stagnant zone boundaries (Nedderman, 1995). Plasticity theory is well established for the prediction of small displacements in granular material and can be extended to the effectively infinite strains in flowing materials. It was later found that the flowing zone predicted by Jenike's radial velocity field is far narrower than that observed in practice (Cleaver and Nedderman, 1993). Many experiments are aimed at investigating types of flow and shapes of the flowing regions. Some factors as: the hopper geometry, height of packed materials, the size of particles, material density, material-wall interface friction influence the shape of flow patterns (Giunta, 1969; Takahashi and Yanai, 1973; Nguyen et al., 1979; Watson and Rotter, 1996; Waters and Drescher, 2000).

Many theoretical works divide steady-state flow (Tüzün and Nedderman, 1982; Graham et al., 1987; Zhang and Ooi, 1998) into two cases: loosely packed material in tall bins; or in shorter bins, but here the bin should be filled continuously. To predict velocities and stagnant boundaries in the flowing material, a few theoretical models are used in such analysis: the rigid perfect plastic model and a kinematic material model (Litwiniszyn, 1963; Mullins, 1972, 1979; Nedderman and Tüzün, 1979; Waters and Drescher, 2000). It was assumed that material density is constant in the

* Corresponding author. Tel.: +48 85 746 9583; fax: +48 85 746 9559.
E-mail addresses: sieliren@pb.bialystok.pl (I. Sielamowicz), sblonski@ippt.gov.pl (S. Blonski), tkowale@ippt.gov.pl (T.A. Kowalewski).

0009-2509/$ - see front matter
doi:10.1016/j.ces.2004.07.135

hopper. Drescher and Ferjani (2004) modelled the evolution of flow zones in cohesionless granular materials introducing a revised kinematic model. They considered stresses developing during the flow and the funnel-type of flow. Weir (2004) developed a new "softening" variable-density plastic flow model and applied it to the steady radial flow of a cohesionless granular material from steep-walled wedge and conical hopper. The flow conditions given by Weir (2004) contains the time derivative of density in order to satisfy mass conservation. Weir (2004) assumed the variation of density with pressure and the variation of density was shown to decrease the mass discharge rate.

The process of discharge is unsteady when the size of the flow region increases with time. The theoretical model for this type of flow assumes an incompressible radial velocity field and kinematic theory (Nedderman, 1995). Considering discharge from a densely packed hopper, a plug flow zone, formed in the material, is observed and it extends upward to the upper surface and then this zone widens and quickly reaches the hopper walls. The boundaries of the flowing zones are shown in figures obtained by DPIV analysis in this paper. In the initial phase of the flow, before reaching the upper surface, the boundaries of the plug flow zone are vertical except near the outlet and the upper surface. In the advanced phase of flow, the flow zone widens and the boundaries become curved. The upper surface changes its shape and becomes concave.

Simulations of the discharge process allow us to understand the material behaviour. The first works (Kvapil, 1959), where two different colours of material were used, allowed detection of zones of flow and the stagnant zones. The flow was observed through the transparent walls of the model to register flow profiles. An X-ray technique was used to look inside the silo. The registered velocities can be seen on the velocity magnitude contours (Lueptow et al., 2000; Ostendorf and Schwedes, 2004; Sielamowicz and Kowalewski, 2004).

Many experimental works have been focused to measure flow patterns. Optical techniques are commonly used in the analysis of velocity profiles near the transparent silo walls. The X-ray technique was frequently applied (e.g. Blair-Fish and Bransby, 1973; Drescher et al., 1978) to obtain information from deeper flow layers.

This paper is devoted to the application of digital particle image velocimetry (DPIV) technique in measurements of evolution of granular material flows in plane flow hoppers. The evolution of the plug flow zone, velocity magnitude contours, velocity vector fields, velocity distributions on certain levels in the model, traces of the single particles are presented in the analysis.

An optical flow technique based on the use of dynamic programming (Quenot et al., 1998) has been applied to particle image velocimetry (PIV) thus yielding a significant increase in the accuracy and spatial resolution of the velocity field. A velocity vector is obtained for every pixel of the image. Calibration carried out for synthetic sequences of images shows that the accuracy of measured displacement is about 0.5 pixel/frame for tested two-image sequences and 0.2 pixel/frame for four-image sequences. The aim of the present investigation is to explore the possibility of using the optical flow technique based on PIV measure velocity in a granular flow.

PIV is a method used for two-dimensional flow structure evaluation. It enables the measurement of the instantaneous in-plane velocity field within a planar section of the flow field, the spatial gradients, dissipation of turbulent energy, spatial correlations, and the like. In the early days of the PIV technique multiple-exposure images and optical auto-spectrum or autocorrelation analysis were applied (Hesselink, 1988). Images taken for PIV analysis were recorded on a film and the flow field was obtained via the computation of the spatial correlation in a small search region. It was a very laborious task to process large number of images. Therefore, an alternative approach—DPIV was introduced (Willert and Gharib, 1991; Westerweel, 1993). Here digital images are recorded directly with a CCD camera and a frame-grabber, and can be studied without the unnecessary delay and overhead associated with the digitisation of photographs. DPIV allows for a simple realization of the cross-correlation technique for pairs of two separate images. The typical DPIV evaluation procedure is based on the analysis of two successive images of the flow. Despite recent progress in the DPIV development further improvement of the accuracy and minimization of the computational time still remains a current research goal (Lourenco and Krothapalii, 1995; Sun et al., 1996). One of the main drawbacks of classical DPIV is its inability to accurately resolve flow regions characterized by large velocity gradients. This is due to the strong deformation of the particle image pattern within a DPIV search window. A group of researchers (Huang et al., 1993; Tokumaru and Dimotakis, 1995; Gui and Merzkirch, 1996)—proposed several alternative evaluation methods to remove the above limitations. It appeared that the optical flow method may be an interesting alternative, offering high evaluation accuracy without most of the typical DPIV limitations. This technique which was developed for detecting the motion of large objects in a real world scene, has been adopted to measure fluid flow (Quenot et al., 1998), yielding a significant increase in the accuracy and spatial resolution of the velocity field.

In this paper, we describe our efforts to apply the optical flow technique DPIV to investigate the dynamic behaviour of a granular material during discharge, and to measure flow profiles, velocity distributions, vector fields in plane flow hoppers with central filling and discharge. The following second paper will be devoted to flows in converging hoppers, and the third to the central and eccentric filling and discharge in plane hoppers.

2. Theory and experiments

Jenike in his models distinguished radial stress fields (RSF) and velocity fields (RVF) and presented the results in a graphical form (Jenike, 1961, 1964). The radial velocity field (RVF) presents a particular solution to the full stress equation for an ideal Coulomb material. The radial velocity field (RVF) is derived from the radial stress field on the assumption that material obeys the principal of coaxiality, sometimes known as the principal of isotropy (Moreea and Nedderman, 1996). The methods built by Jenike can predict the existence of stagnant zones in flowing material. The observations of batch discharge also showed that the position of the stagnant zone boundary changes slowly in time. Because the kinematic model cannot predict the existence of the stagnant zone boundary, therefore the stagnant zone boundary was defined to be the position at which the velocity was equal to 1% of the centreline velocity at the same height (Watson and Rotter, 1996). It was also found as a satisfactory approximation for the steady state. Tüzün and Nedderman (1982) showed that the stagnant zone boundary should be taken to be the stream surface within which 99% of the total flow takes place. Theoretical predictions of the velocities and the flow boundary were based on the use of a purely kinematic model or the rigid perfectly plastic model. Both models assumed the constancy of the material density throughout the bin, i.e., incompressible flow is considered. The kinematic models mentioned above differ slightly in their qualitative aspects but all three describe that the velocity distribution is presented by the differential equation

$$\frac{\partial \upsilon}{\partial y} = B\,\frac{\partial^2 \upsilon}{\partial x^2}, \tag{1}$$

where υ is the vertical velocity and x and y are horizontal and vertical distances, respectively (Nedderman, 1995). As Nedderman (1995) presents, Eq. (1) is not invariant with respect to rotation of coordinates, because the models are concerned with gravity flow and y-coordinate must be directed vertically. The parameter B has the dimension of length and is often taken in the order of particle diameter. Eq. (1) is parabolic and cannot have discontinuous solutions and used only for two-dimensional systems. For cylindrical symmetry, the kinematic model has the form

$$\frac{\partial \upsilon}{\partial z} = \frac{B}{r}\,\frac{\partial}{\partial r}\left(r\,\frac{\partial \upsilon}{\partial r}\right). \tag{2}$$

Watson and Rotter (1996) showed that the streamlines in a discharging cylindrical bunker are indeed similar to those predicted from the kinematic model. Using the finite element method, the solution of Eq. (2) for cylindrical bunkers for many different values of the kinematic constant B was presented and considerable agreement between the predictions and the streamlines in steady flow was shown. Watson and Rotter (1996) recognized three regions in the solution. Plug flow was found in the upper part of the bunker, where the velocity is presented as the ratio—the volumetric flow rate divided by the cross-sectional area. In the region close to the orifice, velocities of passing particles are high. It was also found that the only region where the velocity of the flowing material cannot be predicted is the intermediate region, located far from the orifice and far from the walls. Waters and Drescher (2000) indicated in their paper that the predicted velocities are higher along the centre line and decrease gradually towards the boundary. The shape of the boundary was described as “a growing candlelight”. In the discussion it was shown that the kinematic model gives no information about the stagnant zones (Nedderman, 1995). That is why a new model was proposed assuming that on filling, the material compacts to the initial density and when the process of discharge starts, the material density falls to another value. More details of the above discussion can be found in the literature (Nedderman, 1995). Waters and Drescher (2000) modelled plug flow in bins and proposed a theoretical model (purely kinematic) for describing the evolution of the plug flow zone. They have not considered the evolution of the velocity field and the stress field but only a simplified velocity field. The model relates to axisymmetric flow as well.

3. Experimental setup

One of the first successful attempts to apply the PIV technique to granular matter was described by Waters and Drescher (2000) and Lueptow et al. (2000). Recently Ostendorf and Schwedes (2004), Sielamowicz and Kowalewski (2004), Bohrnsen et al. (2004) reported the use of the PIV technique in their experiments to obtain information on local velocities of particles at several elevations in the densely packed materials. Ostendorf and Schwedes (2004) combined PIV measurements with wall normal stress measurements at different points of time in the large-scale silo.

This paper presents our attempt to use the DPIV technique in measuring cohesionless granular material flows to obtain data on the evolution of plug flow. A series of experiments was conducted in a plane model made of Plexiglas. The optical flow DPIV technique is used to register evolution of the flow, velocity fields and velocity distributions in the granular materials. The development of the flow is evaluated in the model and traces of selected particles in the consecutive stages of the flow. In the following, the selected results obtained for the flat bottomed model are given.

Fig. 1 shows the experimental setup used for the flow analysis. It consisted of a Plexiglas box, a set of illumination lamps, and a high-resolution CCD camera (PCO SensiCam). The 12-bit flow images with resolution of 1280×1024 pixels and maximum frequency of 3.75 Hz were acquired by Pentium 4-based personal computer. Long sequences of 100–400 images were taken at variable time intervals for subsequent evaluation of the velocity fields. The velocity field was evaluated for triplets of images using optical flow

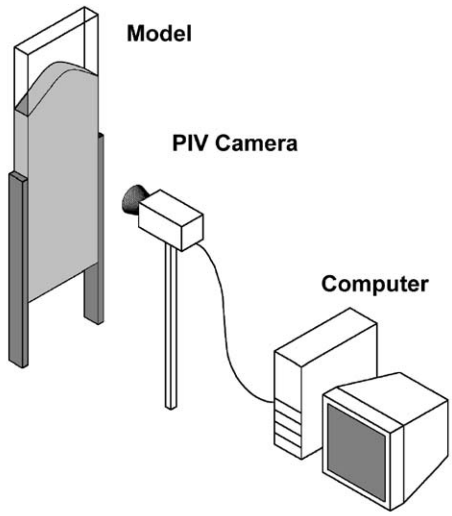

Fig. 1. The experimental setup.

Table 1
Properties of the granular materials used in the experiments

Granular material	Wall friction against Plexiglas	Angle of internal friction	Granular material density deposited through a pipe with zero free-fall
	φ_w (deg)	φ_e (deg)	ρ_b (kg/m^3)
Amarantus	25	28	832 at 1 kPa 833 at 8 kPa
Flax-seed	26	25	746 at 1 kPa 747 at 8 kPa
Buckwheat	28	25	669 at 1 kPa 671 at 8 kPa

PIV technique. Dense velocity fields with vectors for each pixel of the image were obtained and used for further evaluation of the velocity profiles, velocity contours and traces of flowing particles. Intrinsic resolution of the PIV technique is limited by the size of the area of interest that is used in the application of the cross correlation algorithm between subsequent images and this is generally one order of magnitude larger than a single pixel.

The Plexiglas silo model has a height of 80 cm, a depth of 10 cm, and a width of 26 cm. The model was placed on a stand and a granular material was supplied through a box suspended above the model. The construction of the model allowed different inclinations of the silo bottom against the vertical. However, the present description is limited to the flat bottom silo only. The width of the outlet was 1 cm. The bottom of the supplying box had a sieve and the box was filled with granular material to $\frac{2}{3}$ of its height.

Three granular materials were used for the experiments: amarantus, flax-seed and buckwheat. These materials show certain static electricity when flowing and sliding over Plexiglas. Properties of the materials used in the experiments are presented in Table 1. The granular material was introduced through the sieve in the form of a uniform stream into the model of silo to obtain uniform and repeatable packing of the materials with no particle segregation. Before the experiment started, the model was filled with a 78 cm high column of the material.

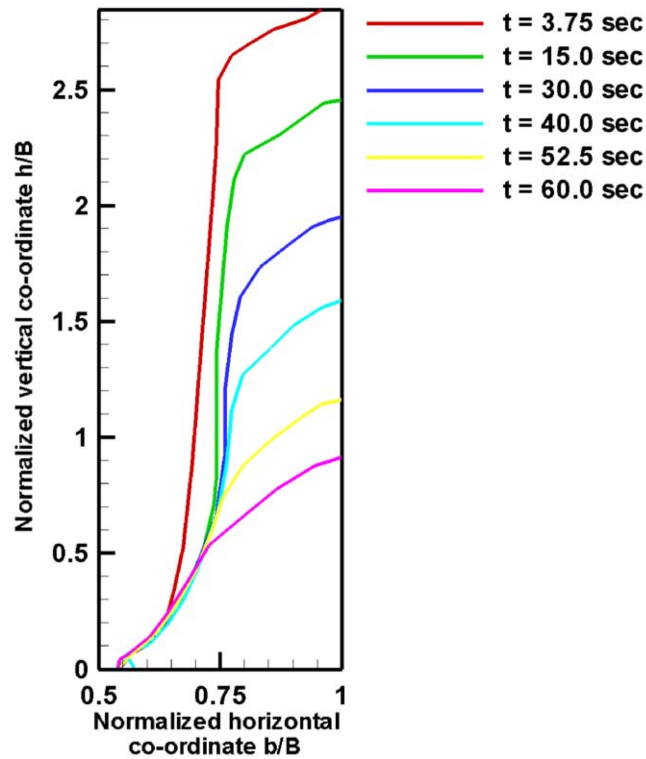

Fig. 2. Experimental measurements of the stagnant boundary—flow of amarantus.

For each experimental run the discharge rate was measured with a digital scale. The velocity fields, the evolution of the flow region and the traces of flowing particles were evaluated from recorded images. Pairs of digital short exposure photographs were taken to describe how the velocity field varied in the flowing material.

Amarantus grain has a shape of regular round balls of 1 mm diameter, straw-coloured. The surface of the grain is plain. Flax-seed has a shape of flattened rotational ellipse 4 mm × 2 mm, brown in colour and plain, brilliant surface. Buckwheat seed is like a pyramid of total height 2 mm. Its surface is not as brilliant as flax-seed, being a little darker brown colour than flax-seed.

4. Selected results

Watson (1993) presented his experimental measurements of the stagnant zone boundary as a function of time obtained in a semi-cylindrical bunker of diameter 650 mm fitted with a semi-circular orifice of diameter 65 mm. Nedderman (1995) showed the predicted position of the stagnant boundary as a function of time. These two investigations indicate that the kinematic model considered by Watson (1993) and Nedderman (1995) give an excellent prediction of the development of the stagnant zone boundary. Some

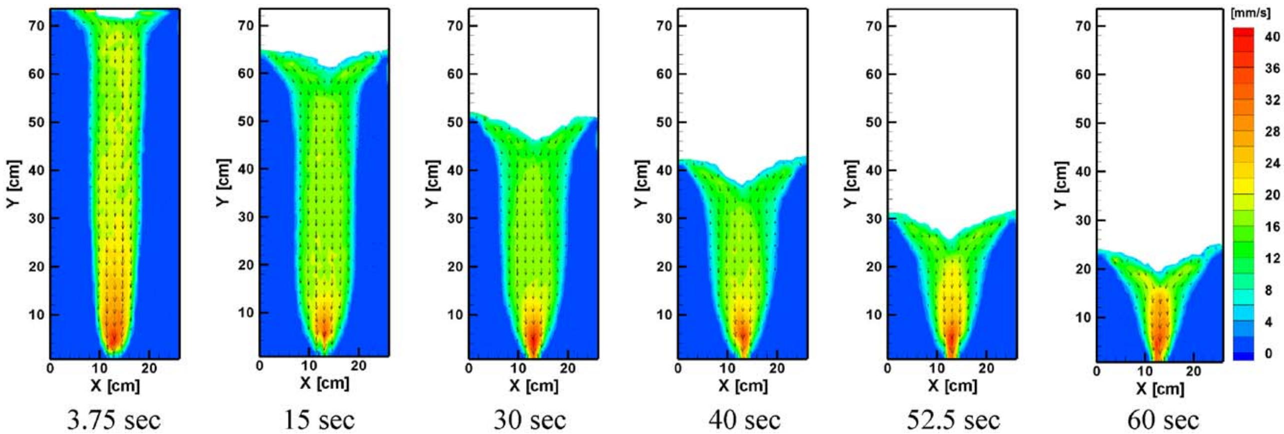

Fig. 3. Velocity fields and velocity magnitude contours in the model of flowing amarantus.

differences were noticed close to the orifice, where the assumption of a point sink differs from the orifice of diameter 65 mm as used in the experiments. In Fig. 2, development of the stagnant boundary resulting from the present experiments is given.

The analysis given in Fig. 2 presents results obtained in the measurements of the stagnant boundaries at the given time steps in the plane model of silo with the angle to vertical 90°. It shows the flow of amarantus seed for one-half of the model. It can be seen that the plug flow develops very quickly in the material with the initial phase reaches after 3.75 s from the beginning of the flow, then the flowing zone rapidly reaches the upper surface. We can say that the flowing zone is similar to funnel flow—internal or pipe flow. Generally, the shape of the flowing zones of amarantus in Fig. 2 is converging in the intermediate phase of the flow similar to that observed in the experiments carried out by Watson (1993) and in the predictions given by Nedderman (1995). However, the lines of the stagnant boundaries in Fig. 2 are closer to each other in their vertical parts. It indicates that the flowing region does not increase in its width as it was observed in Watson (1993) and Nedderman (1995). After the initial time of 3.75 s the material flows gradually from the upper parts into the flowing zone and the stable funnel zone forms. It preserves its width till the end of the flow, in contrast to the results of Watson (1993) and Nedderman (1995) showing gradual widening of the flowing zone with time. It remains unclear as to whether absence of the lateral expansion of the funnel flow is related to particle geometry or to the difference in the initial packing density.

The total time of flow of amarantus was 60 s. In Fig. 2 the horizontal axis is given as a normalised width of the model and the vertical axis as a normalised height of the model.

Fig. 3 presents the velocity fields and velocity magnitude contours of the flowing amarantus obtained from the sequence of 315 images taken at the intervals of 0.2666 s.

Fig. 3 shows the evolution of the plug flow zone during gravitational discharge obtained by PIV measurements. The development of a high-velocity region (red colour contour) at the outlet is clearly visible. The stagnant zones are indicated by the blue colour of the velocity contour map.

At the beginning of the experiment, a plug flow zone in the flow region propagates upward and then widens with height. When the flow region reaches the upper surface, it becomes concave. Shortly one may observe nearly uniform channel flow for the entire height of the silo. As seen in Fig. 3, the upper surface changes its shape while the material flows. The upper surface is almost flat at the beginning of the experiment, but becomes nearly conical in its final stages. In the stagnant zones, the measured velocity is zero. In the plug flow region, the velocity vectors in the initial phase of flow are vertical, indicating absence of measurable lateral displacements. In the upper part of the flow, the velocity vectors indicate converging lateral flow towards the flowing zone. The velocity of the flowing material has its maximum on the axis of the model near the outlet and decreases towards the top and the model walls. The flow profiles are symmetric.

In the advanced phase of the flow, the lateral dimension of the plug flow region increases. In the plug flow region the velocity vectors pass vertically towards the outlet. They have the same length along the symmetry axis and indicate, here, the highest velocities. The flow direction changes near the outlet and the velocity vectors pass directly to the outlet but their traces are not vertical in the whole region. Near the boundaries, the vectors pass along the curved lines. The length of the vectors and the colour of the contour indicate the magnitude of the velocity. Initially, the plug flow width is relatively small. The average flow velocity diminishes with time. The high-velocity flow region is located in the vicinity of the outlet. In the final phase of the flow, the elevated velocity region at the outlet spreads upwards in the plug flow zone.

Fig. 4 presents the traces of selected particles calculated from the velocity field measured in the model for three flowing materials. The traces of flowing particles represent the motion of virtual particles, indicating the flow

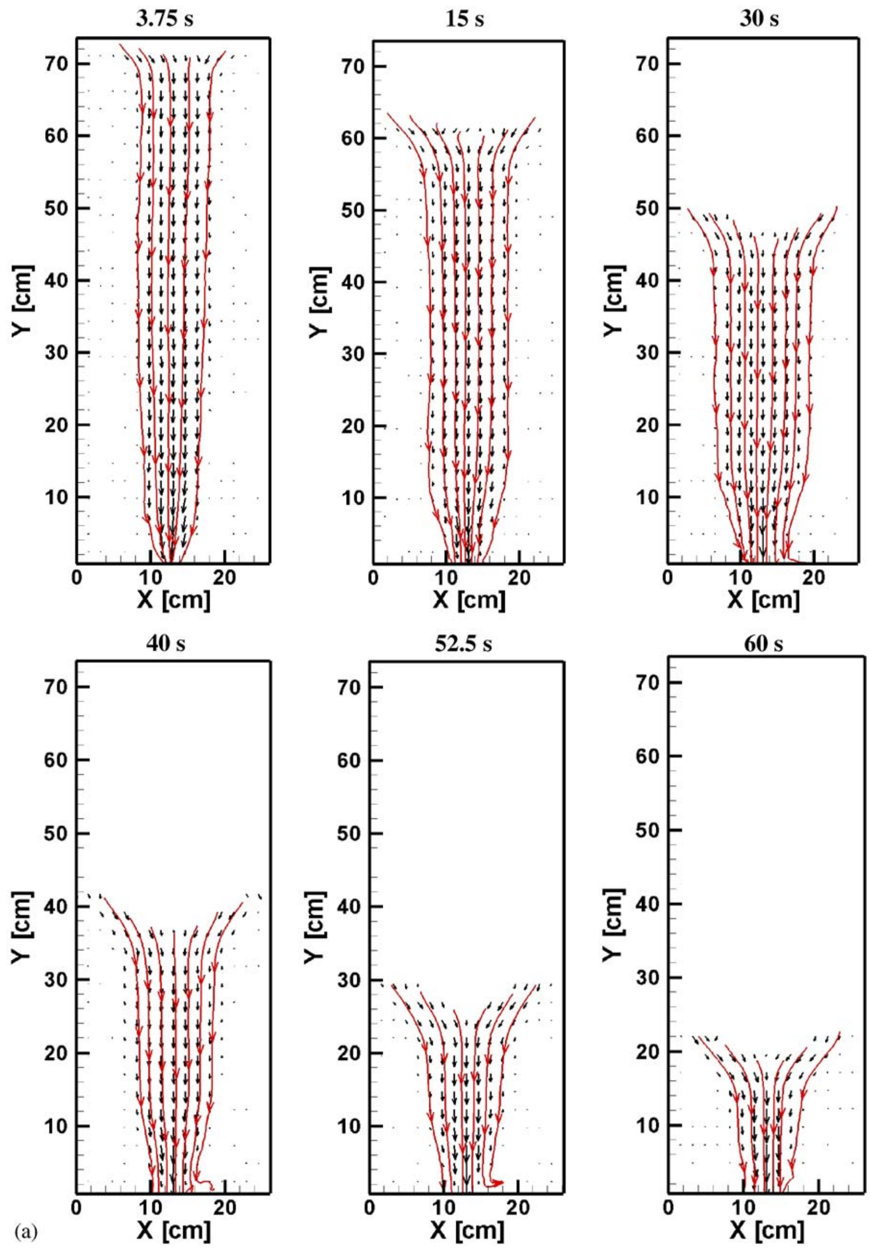

(a)

Fig. 4. Traces of the individual particles of flowing: (a) amarantus; (b) flax-seed; (c) buckwheat.

structure in the flowing zone. Fig. 4a shows the traces obtained for the flowing amarantus. The experimental results of the traces of selected particles are depicted with red vectors. The flow of amarantus is symmetrical but some disturbances of the flow of the single particles, especially near the outlet, can be seen. The black vectors denote the flowing region and the lengths of the vectors denote the velocity. In the stagnant zones there are points which denote vectors of zero value.

Near the outlet, where the velocity is highest, convergence of the flow into the orifice is well illustrated by the traces of the flowing seeds. Local non-uniformities of the velocity field are well reflected in the asymmetry of the traces observed in some regions. It appears that some degree of non-uniformity of the material is unavoidable in the experiments.

In Fig. 4b, c the traces of individual particles for flowing flax seed and buckwheat evaluated at the selected elevations are depicted with red colour. The flowing zone is depicted with black vectors. These six figures are only a part of the results obtained in the experiments. The total flow time for flax-seed was measured as 1 min 43 s and for buckwheat 2 min 2 s. It can be interesting to notice that both the flowing granular materials produce different flow structures as shown in Fig. 4b and c. So the flow of flax-seed and buckwheat plugs most of the geometry and is less converged in the outlet region.

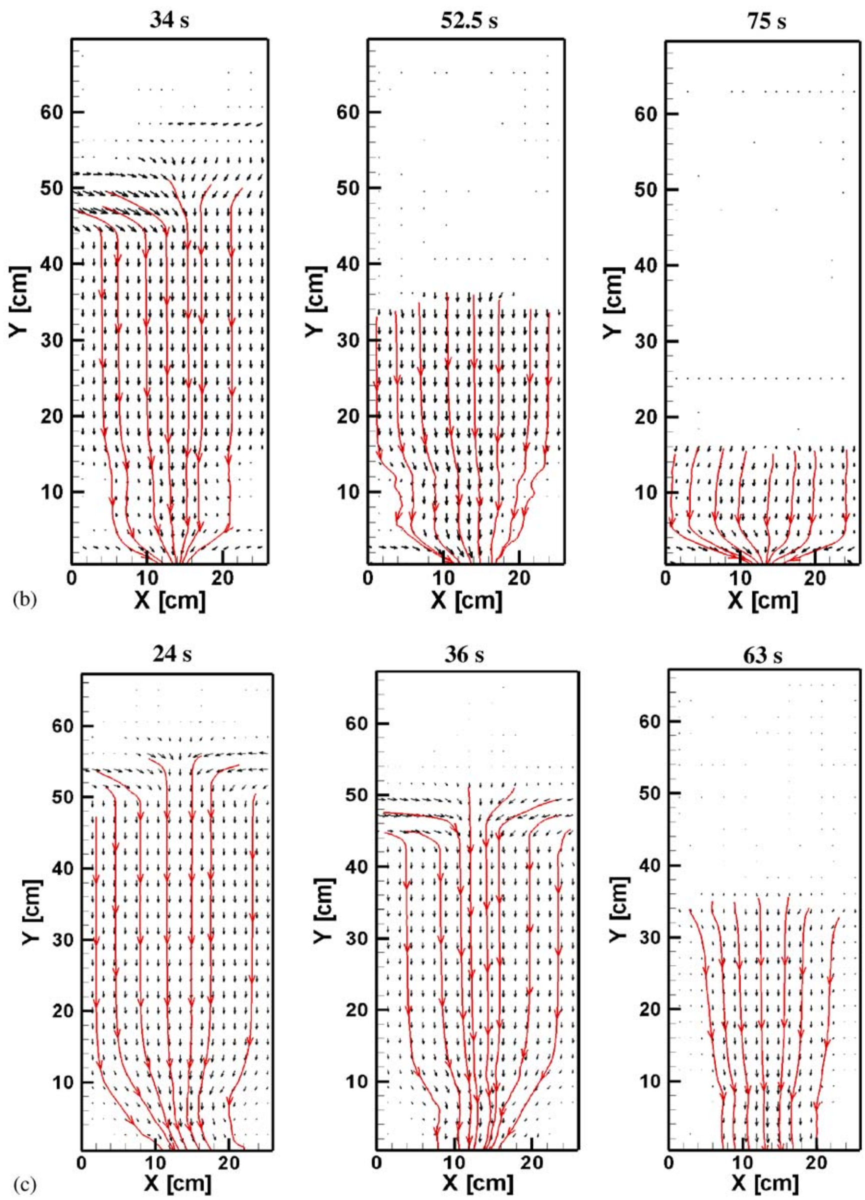

Fig. 4. (*continued*).

The outer traces of flowing particles are close to the boundary lines of the flowing zone. They are not always vertical or smooth. Some irregular lines result because both seeds were less homogeneous and contained some natural pollutions. The shape of the grains, and the kind of seed surface influence its flowing properties.

In Fig. 5, selected velocity profiles of the flowing amarantus are shown. The profiles of the vertical velocity components across the cavity were obtained at different heights (indicated in the legend) and at time steps 3.75, 30 and 52.5 s after the beginning of the experiment. At 5 cm above the outlet (the red line in Fig. 5) the velocity profile is symmetrical. After 30 s the velocity reaches its maximum value 40 mm/s. After 52.5 s a slight symmetry disturbance can be seen in this velocity profile. At 10 cm above the outlet, the maximum value of the vertical velocity is reached after the time of 3.75 s. It can be noticed that above 20 cm from the outlet the velocity maxima reach similar values in the range between 18 and 22 mm/s. After 30 s the velocity profiles measured at the levels $h = 20, 30, 40$ cm are similar.

After 3.75 s similar velocity profiles were obtained for the height of $30, 40, 50, 60$ cm which indicate a nearly uniform flow in the upper regions of the silo. The same can be seen in Fig. 5 at $t = 52.5$ s. There are three levels for $h = 10, 20, 30$ cm, where a bunch of velocity profiles have almost the same values in the range of 20–25 mm/s is observed. The shape of the profiles in the bunch is similar too.

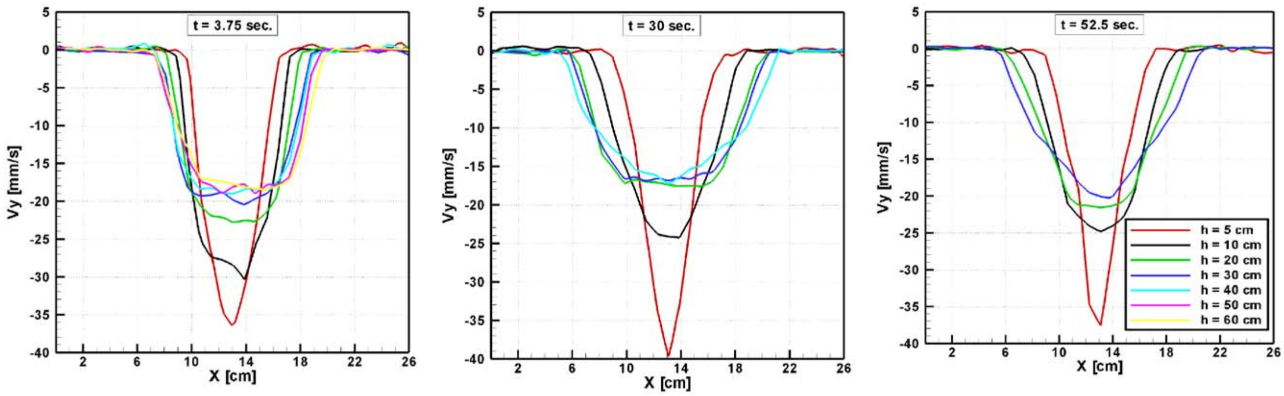

Fig. 5. Velocity profiles for the flow of amarantus seed.

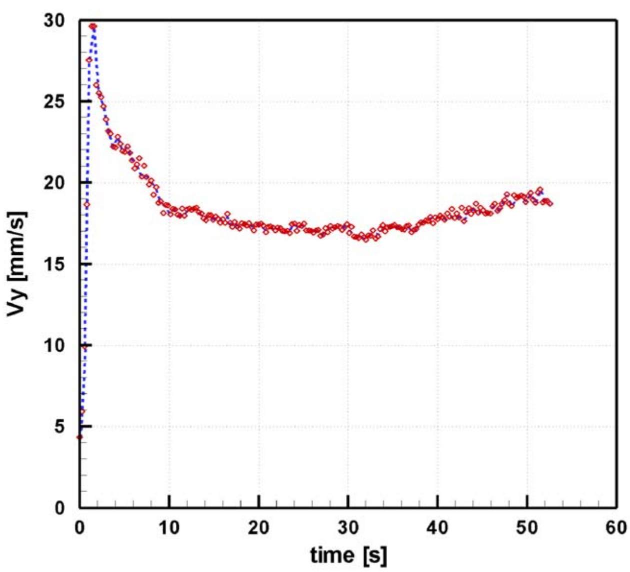

Fig. 6. Evolution of the vertical velocity in the plug flow zone as a function of time, measured at the symmetry axis of the model and height 20 cm for the amarantus seed.

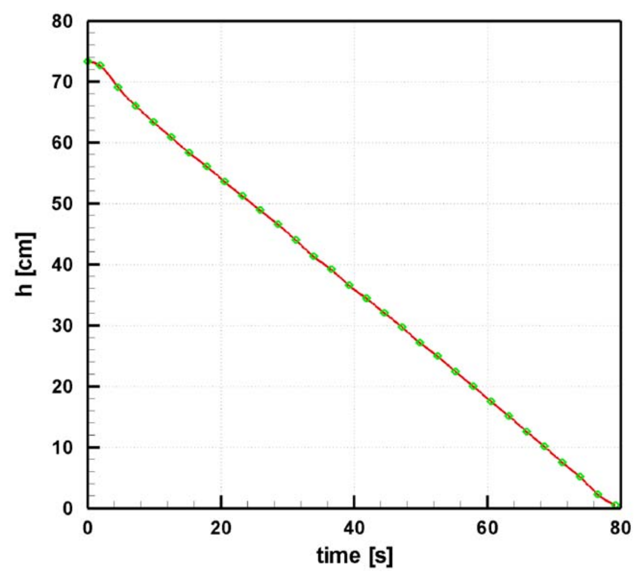

Fig. 7. Evolution of the height of the plug flow zone as a function of time measured at the symmetry axis for the flow of amarantus seed.

Variations in time of the volumetric discharge of granular materials is an important experimental parameter. It can be evaluated from the mean vertical flow velocity and the area of the flowing zone. Figs. 6–8 present the variation of the vertical velocities of particles V_y, the height h and the width $2b$ of the flowing zone of amarantus as a function of time.

Similar diagrams were depicted by Waters and Drescher (2000). Their experiments used a plane flow model made of Plexiglas, 75 cm in height, 26 cm in width and 12.7 cm in depth with the inclination 75° to the vertical. The width of the outlet was 0.5 cm. Crushed walnut shells as a cohesionless material were used in the experiments (Waters and Drescher, 2000). The total flow time was measured for about 250 s. They observed that the maximum velocity of flowing crushed walnut shells was reached shortly after opening the outlet and was about 10 mm/s. Then the velocity decreased and after about 75 s it reduced to 5 mm/s. Similar behaviour was found in the present experiments. Fig. 6 shows that the plug flow velocity reaches its maximum value of 30 mm/s after 2 s. During the first 10 s of the flow, the velocity decreased to the value of 17 mm/s. Between 10 and 40 s the velocity was found to be almost constant with an average value of about 16–17 mm/s. Then, in the advanced phase of the flow the velocity again slightly increased to the value of about 20 mm/s (cf. Fig. 6).

The observed evolution of the plug flow zone is schematically shown in Fig. 7. The height of the plug flow as a function of time (Fig. 7) and the width of the plug flow at the level of 20 cm as a function of time (Fig. 8) are presented.

The height of the plug flow zone was reported by Waters and Drescher (2000) and Drescher and Ferjani (2004) who indicated that the maximum height of the plug flow zone was reached after about 15 s from the beginning of the flow.

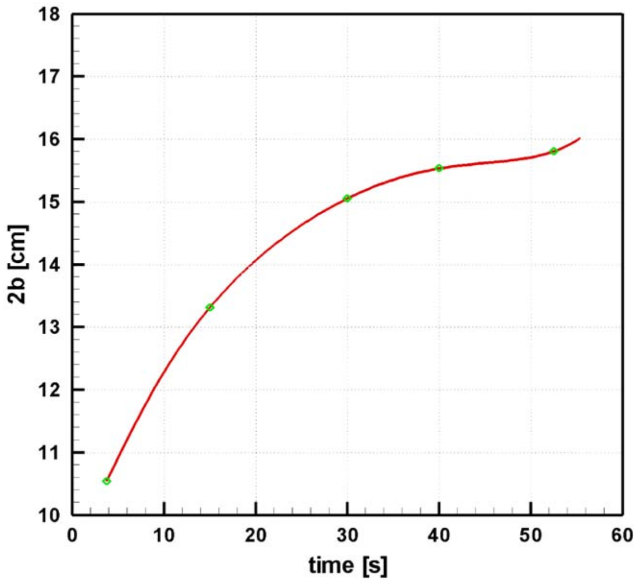

Fig. 8. Evolution of the width of the plug flow zone as a function of time in the symmetry axis at the height 20 cm for the amarantus seed; $2b$—total width of the plug flow zone between the stagnant boundaries.

They found that the plug flow zone reaches the height of the upper surface and then linearly decreases with time. Similar behaviour of the flowing zone was observed in the present experiments (Fig. 7). The evolution of the height of the plug flow can be approximated by linear function of time.

Fig. 8 displays evolution of the width of the plug flow zone as a function of time for the same experiment as in Fig. 7. This experimental analysis confirms the results obtained by Waters and Drescher (2000) who reported the variation of the width of the flowing zone as a function of time for crushed walnut shells. It can be seen that the width of the plug flow zone varies with time and increases. In this experiment, the total width of the plug flow zone at the height 20 cm between the stagnant boundaries was measured. The shape of the function in Fig. 8 is similar to that of Waters and Drescher (2000). The measured width $2b$ in Waters and Drescher (2000) reached its maximal value 0.15 m after about 200 s. In the case of this analysis, the width of the plug flow zone was a little greater and reached a value of about 16 cm after about 30 s of the flow. The width of the plug flow zone rapidly increased in the first 30 s of the flow. After 30 s of the flow the width of the flow zone reached almost its constant value of about 15.5–16 cm. The total time of amarantus flow was measured as 60 s. Relating it to the results obtained by Waters and Drescher (2000) some differences can be encountered. They reported nonlinear increase of the width of the plug flow zone in time. The disparity of the flowing material properties (crushed walnut shells against amarantus seed used here) can be responsible for their different behaviour. Recently, Drescher and Ferjani (2004) showed the experimental results of the evolution of the half-width b of flowing crushed walnut-shells (but in Waters and Drescher (2000) a heavier material was used) as a function of the percentage of mass discharged from the semi-cylindrical bin. They indicated that the variation of b is little effected by the initial height of the material and applies to the influence of half-size outlet. The functions showing the increase of the plug flow zone both in the analysis Waters and Drescher (2000) and of Drescher and Ferjani (2004) are in their general form similar.

The DPIV analysis yields velocity vectors for each point of the flow. This information can be used to predict the stresses in the flowing granular material. Calculating velocities in the flowing region, the derivatives of the obtained velocities and then the stresses can be calculated. In this experimental analysis such calculations were not made though it would be possible to extend this analysis in the future work. Because the issue of stresses both in the flowing material and on the silo walls is very important in the analysis of granular material flows, so further investigations will be done and discussed in the future. Accuracy of DPIV measurements seems sufficient to obtain velocity gradients inside the flowing zone. However, evaluation of the stresses on the bin wall is still a challenging task. The velocity of the granular material near the wall is equal or close to zero and cannot be used to calculate the wall stress. The velocity gradients measured on the boundary of the stagnant zone could offer useful values for calculating wall stress. Such evaluation, combined with the stresses measured at the wall by electrical transducers (Ostendorf and Schwedes, 2004), could offer the possibility to verify theoretical descriptions of mechanical properties of granular media.

5. Conclusions

This paper used the DPIV technique to obtain data on the evolution of the flow in a densely packed, cohesionless materials. The experiments were conducted on a plane flow model made of Plexiglas. The method allowed for an evaluating detailed velocity vector field in the flowing zone and quantitative estimation of its geometry and dynamics. The method appears to be a useful, quantitative diagnostic tool for the study of quasi two-dimensional granular flows. It has the capacity to obtain the stress field within the flowing material.

Acknowledgements

The authors would like to thank the referees for suggestions which led to an improvement of the original manuscript. Many thanks to Professor Zenon Mroz from the Institute of Fundamental Technological Research of Polish Academy of Sciences and Professor Andrew Drescher of the University of Minnesota for their valuable discussion and advice. This paper was partly prepared under the Rector's project W/IIB/13/03.

References

Blair-Fish, P.M., Bransby, P.L., 1973. Flow patterns and wall stresses in a mass-flow bunker. Journal of Engineering for Industry 95, 17–26.

Bohrnsen, J.U., Antes, H., Ostendorf, M., Schwedes, J., 2004. Silo discharge: measurement and simulation of dynamic behaviour in bulk solids. Chemical Engineering Technology 27, 71–76.

Cleaver, J.A.S., Nedderman, R.M., 1993. The measurement of velocity distributions in conical hoppers. Chemical Engineering Science 48, 3703.

Drescher, A., Ferjani, M., 2004. Revised model for plug/funnel flow in bins. Powder Technology 141, 44–54.

Drescher, A., Cousens, T.W., Bransby, P.L., 1978. Kinematics of the mass flow of granular material through a plane hopper. Geotechique 28 (1), 27–42.

Giunta, J.S., 1969. Flow patterns of granular materials in flat-bottom bins. Journal of Engineering for Industry Transactions of the ASME 91, 406–413.

Graham, D.P., Tait, A.R., Wadmore, R.S., 1987. Measurement and prediction of flow patterns of granular solids in cylindrical vessels. Powder Technology 50 (1), 65–76.

Gui, L.G., Merzkirch, W., 1996. A method of tracking ensembles of particle images. Experiments in Fluids 21, 465–468.

Hesselink, L., 1988. Digital image processing in flow visualization. Annual Review of Fluids Mechanics 20, 421–485.

Huang, H.T., Fiedler, H.E., Wang, J.J., 1993. Limitation and improvement of PIV. Part I: limitation of conventional techniques due to deformation of particle image patterns. Experiments in Fluids 15, 168–174.

Jenike, A.W., 1961. Gravity Flow of Bulk Solids. Bulletin 108, University of Utah Engineering Experiment Station.

Jenike, A.W., 1964. Storage and Flow of Solids. Bulletin 123, University of Utah Engineering Experiment Station.

Kvapil, R., 1959. Theorie der Schuttgutbewegung, VEB Verlag Technik, Berlin.

Litwiniszyn, J., 1963. The model of a random walk of particles adopted to researches on problem of mechanics of loose media. Bulletin l'Academie Polonaise Sciences 11, 61–70.

Lourenco, L., Krothapalii, A., 1995. On the accuracy of velocity and vorticity measurements with PIV. Experiments in Fluids 18, 421–428.

Lueptow, R.M., Akonur, A., Shinbrot, T., 2000. PIV for granular flows. Experiments in Fluids 28 (2), 183–186.

Moreea, S.B.M., Nedderman, R.M., 1996. Exact stress and velocity distributions in a cohesionless material discharging from a conical hopper. Chemical Engineering Sciences 51 (16), 3931–3942.

Mullins, W.W., 1972. Stochastic theory of particle flow under gravity. Journal of Applied Physics 43, 665–677.

Mullins, W.W., 1979. Critique and comparison of two stochastic theories of gravity-induced particle flow. Powder Technology 23, 115–119.

Nedderman, R.M., 1995. The use of the kinematic model to predict the development of the stagnant zone boundary in the batch discharge of a bunker. Chemical Engineering Science 50, 959–965.

Nedderman, R.M., Tüzün, U., 1979. A kinematic model for the flow of granular materials. Powder Technology 22, 243–253.

Nguyen, T.V., Brennen, C., Sabersky, R.H., 1979. Gravity flow of granular materials in conical hoppers. Journal of Applied Mechanics, Transactions of the ASME 46, 529–535.

Ostendorf, M., Schwedes, J., 2004. Application of optical measurement techniques on the investigation of bulk solids flow behaviour in silos. International Congress for Particle Technology, Partec 2004, Nurnberg, Germany, 16–18 March.

Quenot, G.M., Pakleza, J., Kowalewski, T.A., 1998. Particle image velocimetry with optical flow. Experiments in Fluids 25, 177–189.

Sielamowicz, I., Kowalewski, T.A., 2004. DPIV technique in modelling granular material flows in a model of silo made of Plexiglas. International Congress for Particle Technology, Partec 2004, Nurnberg, Germany, 16–18 March.

Sun, J.H., Yates, D.A., Winterbone, D.E., 1996. Measurements of the flow field in a diesel engine combustion chamber after combustion by cross-correlation of high-speed photographs. Experiments in Fluids 20, 335–345.

Takahashi, H., Yanai, H., 1973. Flow profile and void fraction of granular solids in a moving bed. Powder Technology 7, 205–214.

Tokumaru, P.T., Dimotakis, P.E., 1995. Image correlation velocimetry. Experiments in Fluids 19, 1–15.

Tüzün, U., Nedderman, R.M., 1982. Investigation of the flow boundary during steady-state discharge from a funnel-flow bunker. Powder Technology 31 (1), 27–43.

Waters, A.J., Drescher, A., 2000. Modeling plug flow in bins/hoppers. Powder Technology 113, 168–175.

Watson, G.R., 1993. Flow patterns in flat bottomed silos. Ph.D. Thesis, University of Edinburgh.

Watson, G.R., Rotter, J.M., 1996. A finite element kinematic analysis of planar granular solids flow. Chemical Engineering Science 51, 3967–3978.

Weir, G.J., 2004. A mathematical model for dilating, non-cohesive granular flows in steep-walled hoppers. Chemical Engineering Science 59, 149–161.

Westerweel, J., 1993. Digital particle image velocimetry—theory and application, Delft University Press,

Willert, C.E., Gharib, M., 1991. Digital particle image velocimetry. Experiments in Fluids 10, 181–193.

Zhang, K.F., Ooi, J.Y., 1998. A kinematic model for solids flow in flat-bottomed silos. Geotechnique 48 (4), 545–553.